1-1-2021

Ecohydrology of Epiphytes: Modelling Water Balance, CAM Photosynthesis, and Their Climate Impacts

Gretta Miller
Princeton University

Samantha Hartzell
Portland State University, s.hartzell@pdx.edu

Amilcare Porporato
Princeton University.

Citation Details

Miller, G., Hartzell, S., & Porporato, A. Ecohydrology of epiphytes: modeling water balance, CAM photosynthesis, and their climate impacts. Ecohydrology, e2275. https://doi.org/10.1002/eco.2275

Ecohydrology of epiphytes: modeling water balance, CAM photosynthesis, and their climate impacts

Greta Miller[1,2], Samantha Hartzell[1,3] & Amilcare Porporato[1,4]

Submitted to *Ecohydrology*

[1]Department of Civil and Environmental Engineering, Princeton University, USA

[2]Department of Civil and Environmental Engineering, University of California, Berkeley, USA

[3]Department of Civil and Environmental Engineering, Portland State University, Portland, USA

[4]Princeton Environmental Institute, Princeton University, USA

Corresponding Author: Amilcare Porporato (aporpora@princeton.edu)

Abstract

Epiphytes are aerial plants, often characterized by CAM (Crassulacean Acid Metabolism) photosynthesis, which make up a significant portion of the biomass in some rainforests. Their unique characteristics have not yet been included in ecohydrological models and their potential impact on local hydrometeorology is largely unexplored. This work introduces a water balance model for epiphytes, which adapts the soil-plant-atmosphere continuum model to represent a plant system without soil and couples it to the Photo3 photosynthesis model, which includes CAM photosynthesis. The model, which is parameterized with field data of *Guzmania monostachia*, accurately captures the observed hydraulic and photosynthetic behavior of the epiphytic species. The application of vertical profiles of environmental inputs within the rainforest canopy shows increasing transpiration rates and decreasing water use efficiency with increasing canopy height, which corresponds to observed distributions of epiphytes in rainforests. Given that vascular epiphytes constitute a maximum of 35-50% of the foliar biomass in rainforests and contribute up to 13% of forest net primary production, they may contribute up to 10-50% of total rainforest evapotranspiration, a significant portion of the water cycle on the local ecosystem scale. The results of this work provide a missing piece to current ecohydrological models, and can be integrated into Earth system models to help improve the physical representation of transpiration and free-surface evaporation from canopy, in current and future climates.

Keywords (8)

epiphyte, Crassulacean acid metabolism (CAM) photosynthesis, evapotranspiration, plant hydraulics, plant water storage, modeling, rainforests

1 Introduction

Understanding and quantifying the mechanisms through which water moves through plants in the natural environment remains a central question in ecohydrology. Physiologically based plant models, which are used to quantify soil uptake and transpiration, typically model water fluxes through the soil-plant-atmosphere continuum. However, models for vascular epiphytes, which do not root in the soil, have not yet been developed or integrated into plant models. Accurately quantifying the water fluxes through epiphytes would greatly improve our understanding of their role in rainforests, arid ecosystems, and the larger global water cycle.

Epiphytes, by definition, grow non-parasitically on other plants, living on trunks and branches of trees in the canopy. In contrast to plants that live in the soil, epiphytes obtain water and nutrients directly from the precipitation, air, and debris in their surrounding environment. Epiphytes have been shown to exhibit marked differences in both leaf structure and water relations from hemiepiphytes, their soil-rooting growth form (Holbrook & Putz, 1996). Globally, there are an estimated 28,000 species of vascular epiphytes, which occur mostly in tropical regions (Zotz, 2016). In rainforest ecosystems, vascular epiphytes are locally abundant and highly diverse, and they fill important ecological niches, where they optimize space availability and often inhabit drier microareas within the canopy. Due to their drought tolerance and water use efficiency, epiphytes also live in arid and semi-arid ecosystems. Epiphytes can affect the water budget of their environment by changing the interception and water storage within the watershed, which indirectly affects soil moisture (Pypker et al., 2006; Stanton et al., 2014). They can also affect the microclimate by buffering temperature fluctuations and reducing the daytime vapor pressure deficit (Stanton et al., 2014).

Studies have shown that the most relevant abiotic constraint for the growth and vegetative function of epiphytes is water shortage (Zotz & Hietz, 2001). Epiphytes can obtain water from rain, dew, water vapor in the atmosphere, and stem runoff from their host. Water uptake and storage processes in epiphytes involve tank storage, absorptive structures such as trichomes and velamen, and large water storage capacitances in the plant tissue. Epiphyte tanks are water-impounding storage containers on the surface of the plants between the stem and the leaves that help to compensate

for access to soil moisture (Zotz & Thomas, 1999). The water balance of the tank depends on the tank capacity, the catchment area of the plant, and aspects of the plant geometry that influence evaporation (Zotz & Thomas, 1999). Trichomes are multicellular, hair-like structures located in concavities on the leaf surface that absorb liquid water, water vapor, and nutrients from the atmosphere (Schmitt et al., 1989). Velamen, which are root-like structures, often serve to anchor the epiphyte to its location, and can assist in absorbing water and nutrients from their environment as well (Zotz, 2016). Epiphytes can also have a large water storage capacitance in their plant tissue, allowing for long-term water storage between intermittent precipitation events (Martin & Schmitt, 1989). In addition, many species of epiphytes use CAM photosynthesis, a water-preserving photosynthetic pathway in which they minimize water loss by closing their stomata during the day and opening them at night when atmospheric vapor pressure deficits are lower (Benz & Martin, 2006; Zotz, 2004). Facultative C3-CAM plants can reversibly induce CAM during dry periods to prolong higher net carbon gain at lower water cost (Winter & Holtum, 2014). Silvera and Lasso (2016) estimate that up to 50% of tropical epiphytic species exhibit some degree of CAM photosynthesis, and Lüttge (2004) estimates that approximately 57% of vascular epiphytes are CAM plants.

According to Schlesinger and Jasechko (2014), tropical rainforests make up 16% of Earth's land cover and receive an average of 1830 mm of precipitation per year, representing 35% of total terrestrial precipitation. Based on data from MODIS and FAO models, tropical rainforests account for 28.5 - 33.1% of terrestrial evapotranspiration (927-1076 mm/yr), and transpiration accounts for 70 $\pm$14% of the total evapotranspiration (T/ET ratio) in tropical rainforests (Schlesinger & Jasechko, 2014). On average, vascular epiphytes make up about 20% of the foliar biomass in rainforests and montane forests of past studies (Zotz, 2016), but can make up to 35-50% of the foliar biomass (Lüttge, 2004; Nadkarni, 1984), and contribute up to 13% of forest net primary production (Richardson et al., 2000). Since epiphytes account for a significant portion of the foliar biomass of some rainforests, they likely account for a large portion of the water budget in rainforests. Thus, they may also make up a significant proportion of the total terrestrial evapotranspiration, and have an impact on the global water fluxes modeled in climate and vegetation models. However, Earth system models do not currently integrate epiphytes into the vegetation components of their models, so the estimates of transpiration, free-surface evaporation from canopy, soil moisture, and T/ET

ratio may be less accurate. Since rainforests are important ecosystems for both the global water and carbon balances, a better physical representation of epiphyte behavior into the modeling of rainforest systems could impact the timing and magnitude of water and carbon fluxes.

Some developments in plant modeling have included limited epiphytic characteristics. For example, Mu et al. (2011) improved the MODIS evapotranspiration algorithm by including nighttime transpiration (i.e., cuticular transpiration) and evaporation from the water intercepted by the surface of the canopy. Past studies on modeling the hydrological process of epiphytes have focused on specific epiphytic species in certain locations and models of particular components of epiphytes. For example, Jarvis (2000) integrated cloud deposition and interception from epiphytes into a hydrological model of a montane cloud forest in Colombia. Zotz and Thomas (1999) developed model calculations for tank water storage of bromeliads. Despite these advances, the unique hydrological characteristics of epiphytes have not yet been developed into a plant hydraulic model.

As a first step towards a more accurate quantification of epiphyte water fluxes, this work introduces a comprehensive water balance model for vascular epiphytes. The hydrological model is coupled with a photosynthesis model, Photo3, to represent both the C3 and CAM photosynthesis common in epiphytes (Hartzell et al., 2018). To model the water balance, the soil-plant-atmosphere continuum model from past studies is adapted to represent a plant system without soil. The model incorporates epiphytic characteristics including water-impounding tanks, absorptive structures such as trichomes and velamen, succulent properties, and the omission of root water uptake.

In this work, the model was parameterized for *Guzmania monostachia*, an epiphytic tank bromeliad commonly known as a West Indian tufted airplant which performs C3 and facultative CAM photosynthesis. The parameterized model is then verified with experimental data from two past studies of transpiration and carbon assimilation in *G. monostachia* with primarily C3 photosynthetic behavior. Finally, the hydraulic behavior of a single tank CAM epiphyte in dry-down conditions and the variation at different heights in a vertical canopy structure are explored. The model accurately captures the hydraulic and photosynthetic behavior of epiphytes, while also high-

lighting the need for more studies and modeling of epiphytes for future applications in climate modeling, ecological studies, and water resources engineering.

2 Methods

2.1 Overview of Model

The epiphyte model characterizes the main water fluxes and storages in epiphytes, as shown in Figure 1. In the water balance, there are two water storages: external tank storage and internal plant capacitance. The tank storage gains water from interception of precipitation, and loses water from free-surface evaporation and uptake from the plant. Water enters the epiphyte through uptake from trichomes, uptake from roots (e.g., velamen), and uptake from the tank. Water exits the epiphyte through transpiration from the stomata.

The epiphyte model is coupled to Photo3, which is a photosynthesis model that represents the C3, C4, and CAM photosynthetic pathways in a consistent, physiologically based manner (Hartzell et al., 2018). Photo3 includes the Farquhar et al. (1980) model for photosynthetic carbon demand, an optimal control model for stomatal conductance (Buckley & Schymanski, 2014; Katul et al., 2009; Medlyn et al., 2011), and a model of the soil-plant-atmosphere continuum for plant hydraulics (Hartzell et al., 2018). For CAM photosynthesis, the photosynthetic C3 core is coupled with a model for carbon fixation that is temporally separated from the Calvin cycle (Hartzell et al., 2018).

To capture the dynamics of the water fluxes through epiphytes, the epiphyte model follows an approach similar to the resistor-capacitor model of the soil-plant-atmosphere continuum (Hartzell et al., 2017, 2018; Hunt et al., 1991; Nobel & Jordan, 1983; Tyree & Ewers, 1991), without the soil component, and with the addition of schemes for external tank water storage and absorption of atmospheric water vapor through trichomes and velamen in humid conditions. The hydraulic model is a big-leaf plant model with an internal and external water storage capacity. Given inputs

of air temperature, solar radiation, and specific humidity, the model estimates transpiration, carbon assimilation, and other hydraulic and photosynthetic variables.

2.2 Model Implementation

Environmental inputs to the epiphyte model include solar radiation (ϕ), specific humidity (q_a), and air temperature (T_a). Precipitation can either be provided as an input, set to 0 to simulate a dry-down, or generated stochastically in the model. Outputs of the model include hydraulic characteristics such as leaf water potential, and water balance processes such as transpiration, free-surface tank evaporation, and changes in tank storage. The model operates on a 30-minute time step to capture the strong dependence of CAM photosynthesis on variability in environmental conditions (Hartzell et al., 2018). For all simulations, the model has a spin up period of at least one day, in which it is forced with constant conditions (relative plant capacitance, relative tank water content, etc.) that are equal to the initial conditions given as inputs to the model. This allows the initial photosynthetic and hydraulic parameters to reach equilibrium before the model begins to output data.

The epiphyte model is currently parameterized with hydraulic and photosynthetic properties for *Guzmania monostachia*, a facultative C3-CAM tank epiphyte shown in Figure 1. *G. monostachia* typically exhibits C3 photosynthesis, but can exhibit CAM photosynthesis in response to stresses such as drought and high light (Pierce et al., 2002). The epiphyte has a wide geographic distribution in the tropics, from southern Florida through Peru and Bolivia, and is usually distributed throughout the upper canopy in rainforests (Zotz & Andrade, 1997). This species was selected because it is a well-studied epiphyte that lives in rainforest ecosystems, and it has important hydraulic characteristics (external tank storage) and photosynthetic characteristics (facultative C3-CAM photosynthesis) that can be used to study plant hydraulic and photosynthetic behavior in the rainforest canopy. The plant parameters for *G. monostachia* are meant to represent the epiphyte at maturity, and are considered constant over the model duration.

2.3 Plant Hydraulics

In the model, which is represented in Figure 2, water moves along a water potential gradient from the tank storage, through the plant, and into the atmosphere. The fluxes of water, including flux from tank (q_t), flux from internal plant capacitance (q_w), transpiration into atmosphere (T), and absorption of atmospheric water vapor (q_h), are equivalent to the conductance (g) multiplied by the difference in water potential (ψ) between each pair of nodes of the plant.

For consistency within the model, all water fluxes are expressed on a per unit ground area basis. Fluxes commonly determined on a per unit leaf area basis, such as transpiration, are converted to a per unit ground area basis with the leaf area index (LAI), which has units of m^2_{leaf} / m^2_{ground}. Fluxes determined on a per unit tank area basis, such as free-surface evaporation from the tank, are converted to a per unit ground area basis with the tank area index (TAI), which has units of m^2_{tank} / m^2_{ground}. The model represents an epiphyte at the plant scale, in which the area of the ground equals the area of the plant. To scale the model to the ecosystem scale, the model results should be multiplied by the ratio of epiphyte area to forest area.

The transpiration flux (T) is a function of the difference between the specific humidity internal to the leaf and the specific humidity of the atmosphere, i.e.,

$$T = g_{sa}\, LAI\, \frac{\rho_a}{\rho_w}(q_l(T_l, \psi_l) - q_a), \tag{1}$$

where $g_{sa}\, LAI$ is the series of the atmospheric and stomatal conductances normalized to a unit of ground area by the leaf area index, ρ_a is the density of air, ρ_w is the density of water, q_l is the specific humidity inside the stomata given as a function of the leaf temperature (T_l) and leaf water potential (ψ_l) (see Appendix A), and q_a is the specific humidity of the atmosphere.

When the humidity of the atmosphere is greater than the humidity of the leaf, water vapor from the atmosphere can be absorbed by the stomata or trichomes on the leaves of the epiphyte. The flux from the humid atmosphere into the leaf (q_h) is a function of the specific humidity internal

to the leaf and the specific humidity of the atmosphere, i.e.,

$$q_h = g_h \, LAI \, \frac{\rho_a}{\rho_w}(q_a - q_l(T_l, \psi_l)), \tag{2}$$

where $g_h \, LAI$ is the conductance of the absorption of atmospheric water vapor normalized to a unit of ground area by the leaf area index, ρ_a is the density of air, ρ_w is the density of water, q_a is the specific humidity of the atmosphere, and q_l is the specific humidity inside the stomata.

Many epiphytes are succulents with an internal plant capacitance. Following Bartlett et al. (2014) and Hartzell et al. (2017), the internal plant water storage is modeled as a concentrated storage, with adjustable parameter f representing the fraction of the plant resistance below the storage branch connecting to the xylem node of the plant (see Figure 2). In this model, it is assumed that the storage is located at mid-plant ($f = 0.5$). The flux between the internal plant capacitance and the xylem (q_w) is a product of the storage conductance and water potential gradient, i.e.,

$$q_w = g_w \, LAI \, (\psi_w - \psi_x), \tag{3}$$

where $g_w \, LAI$ is the storage conductance normalized to a unit of ground area by the leaf area index, ψ_w is the water potential of the internal storage, and ψ_x is water potential of the xylem node.

The internal plant capacitance can be determined through the balance equation, i.e.,

$$LAI \, Z_w \frac{dx_w}{dt} = q_w = q_t + q_h - T, \tag{4}$$

where $LAI \, Z_w$ is the total available water storage depth normalized to a unit of ground area by the leaf area index, x_w is the relative water content in the plant, q_w is the flux from the internal plant storage, q_t is the flux from the tank, q_h is the absorption of atmospheric water vapor, and T is transpiration.

The flux from the tank storage (q_t) is a product of the tank conductance and water potential gradient, i.e.,

$$q_t = g_{tpf} \, (\psi_t - \psi_x), \tag{5}$$

where g_{tpf} is the series of storage and plant conductances to the relative plant height f, ψ_t is the water potential of the tank, and ψ_x is the water potential of the xylem node. When the tank is not empty, the water potential of the water in the tank (ψ_t) is assumed to be 0 MPa since it is free-standing water. The water potential of the internal storage (ψ_w) is given as a function of the pressure-volume curve (see Appendix C). The water potential at the xylem connection node (ψ_x) can be eliminated from Equations 3 and 5 by considering the water flux between the storage and leaf nodes (solving Equation 8 for ψ_x) .

The free-surface evaporation flux from the epiphyte tank (E) is a function of the difference between the saturated specific humidity and the specific humidity of the atmosphere, i.e.,

$$E = g_a \, TAI \, \frac{\rho_a}{\rho_w}(q^*_{sat}(T_t) - q_a), \tag{6}$$

where $g_a \, TAI$ is the atmospheric conductance normalized to a unit of ground area by the tank area index, ρ_a is the density of air, ρ_w is the density of water, q^*_{sat} is the saturated specific humidity at tank temperature (T_t) (see Appendix A), and q_a is the specific humidity of the atmosphere. The temperature of the water in the tank was assumed to be an average of the leaf temperature and atmospheric temperature ($T_t = (T_l + T_a)/2$).

The tank storage can be determined through the balance equation, i.e.,

$$TAI \, Z_t \frac{dx_t}{dt} = R(t) - E - q_t, \tag{7}$$

where $TAI \, Z_t$ is the maximum tank depth normalized to a unit of ground area by the tank area index, x_t is the relative fraction of tank storage with water, $R(t)$ is the rainfall per unit ground area that falls on the epiphyte and enters the tank, E is the free-surface evaporation from the tank, and q_t is the uptake of tank water to the epiphyte. The rainfall ($R(t)$) can be entered as a model input, set to 0 to simulate a dry-down, or generated in the model as a stochastic marked Poisson process with a set mean rainfall frequency (λ) and mean rainfall depth (α).

In addition, the fluxes through the leaf (transpiration and absorption of atmospheric water vapor) must be equal to the fluxes through the plant (flux from the tank and flux from the internal

plant capacitance). Thus, the difference between the transpiration flux (T) and the absorption of atmospheric water vapor (q_h) is a product of the plant conductance and water potential gradient, i.e.,

$$T - q_h = g_{pf}\, LAI\, (\psi_x - \psi_l), \tag{8}$$

where $g_{pf}\, LAI$ is the plant conductance normalized to a unit of ground area by the leaf area index from the relative plant height f, ψ_x is the water potential of the xylem node, and ψ_l is the water potential of the leaf.

To solve the water balance of the epiphyte, the flux leaving the leaf node through transpiration is equal to the flux of water entering the leaf node, i.e.,

$$T = q_w + q_t + q_h, \tag{9}$$

where T is transpiration, q_w is the flux from the internal plant storage, q_t is the flux from the tank, and q_h is the absorption of atmospheric water vapor.

The system of water flux equations are connected with the equation for the energy balance of the plant system, which equates the incoming solar radiation to the outgoing sensible heat and latent heat fluxes, i.e.,

$$\phi = g_a\, \rho_a\, c_p\, (T_l - T_a) + \lambda_w\, \rho_w\, (T - q_h), \tag{10}$$

where ϕ is the net incoming solar radiation, g_a is the atmospheric conductance, ρ_a is the density of air, c_p is the specific heat of air, T_l is the leaf temperature, T_a is the atmospheric temperature, λ_w is the latent heat of vaporization, ρ_w is the density of water, T is the transpiration from the leaf, and q_h is the absorption of atmospheric water vapor. To simplify the model, the plant was considered as its own thermodynamic system. The tank was not considered to be a part of the plant system.

Combining Equations 1, 2 , 5, and 3 into Equation 9 gives the water balance for the epiphyte as a function of the unknowns, ψ_l and T_l. Given the water balance and the energy balance from Equation 10, the system of equations can be solved for ψ_l and T_l.

2.4 Model Parameterization

The model was parameterized for *G. monostachia*, a facultative epiphytic tank bromeliad. The plant hydraulic parameters for *G. monostachia* are shown in Table 1.

The tank area index (TAI) was estimated from empirical equations from Zotz and Thomas (1999). In the study, Zotz and Thomas (1999) give both the projected area of the plant onto the ground (A_{proj}) and the projected area of the tank (A_{tank}) as a function of the dry weight of the plant for *G. monostachia*, i.e.,

$$A_{proj} = \frac{34.67\,W}{1+0.086\,W}, \tag{11}$$

and

$$A_{tank} = \frac{5.57\,W}{1+0.072\,W}, \tag{12}$$

where the areas (A_{proj} and A_{tank}) are in cm^2, and the dry weight of the plant (W) is in g. Assuming a mean dry weight of 10 g for a mature *G. monostachia* plant, the ratio of A_{tank} to A_{proj}, or TAI, is 0.17 $\mathrm{m}^2_{\mathrm{tank}}$ / $\mathrm{m}^2_{\mathrm{ground}}$.

The maximum tank depth (Z_t) was also estimated from empirical equations from Zotz and Thomas (1999). In the study, Zotz and Thomas (1999) give the maximum tank water content (C_{tank}) as a function of the dry weight of the plant for *G. monostachia*, i.e.,

$$C_{tank} = \frac{5.48\,W}{1+0.013\,W}, \tag{13}$$

where the maximum tank water content (C_{tank}) and the dry weight of the plant (W) are in g. Assuming a mean dry weight of 10 g for a mature *G. monostachia* plant, and given the maximum tank water content (C_{tank}) from Equation 13 and the area of the tank (A_{tank}) from Equation 12, the maximum tank depth is 0.015 m.

The maximum plant capacitance depth (Z_w) was estimated from empirical equations from Zotz and Andrade (1997). In the study, Zotz and Andrade (1997) give the maximum plant water

content (PWC) as a function of the dry weight of the plant for *G. monostachia*, i.e.,

$$PWC = 1.50 + 4.99\,W, \tag{14}$$

where the maximum plant water content (PWC) and the dry weight of the plant (W) are in g. Assuming a mean dry weight of 10 g for a mature *G. monostachia* plant, and given the maximum plant water content (PWC) from Equation 14 and the area of the plant (A_{plant}) from Equation 11, the maximum plant capacitance depth is 0.0027 m.

The remaining plant hydraulic parameters in Table 1 are based on values given in past experimental studies or estimates given in existing models. The tank conductance (g_t) is not given in past literature, but was estimated to be similar to soil conductances for rooting plants. The shape parameters (d_1 and d_2) and the total moles of solute (n_s) were determined by fitting a pressure-volume curve to observed data with a nonlinear plant capacitance equation (see Figure 3). The plant capacitance is the sum of the osmotic pressure (Ω) and turgor pressure (Π) (see Appendix C). Several of the plant photosynthetic parameters for the CAM species in Photo3 (Hartzell et al., 2018) were adjusted to fit observed data from Zotz and Andrade (1997) and Pierce et al. (2002) for *G. monostachia*. The adjusted photosynthetic parameters are given in Table 2.

Model results were compared to a study by Zotz and Andrade (1997) measuring water loss in natural conditions during drought. In the study, 16 *G. monostachia* plants of various sizes were used. The plants began well-watered (x_w= 1.0), but without an initial tank water content (x_t= 0). Then the plants were allowed to dry under natural conditions, and were weighed daily at noon to measure water loss, which was assumed to be equal to daily transpiration rates. Because the plants were under well-watered conditions before the start of the experiment, and because *G. monostachia* only exhibits some, but not full CAM behavior in response to stresses (Pierce et al., 2002), the plant was modeled as a C3 plant.

The study by Zotz and Andrade (1997) was conducted in a clearing outside on Barro Colorado Island, Panama in February 1995. Since specific environmental conditions were not provided by Zotz and Andrade (1997), the environmental inputs for the model were obtained from the February

1995 weather data from the Lutz meteorological tower on Barro Colorado Island, from the Physical Monitoring Program of the Smithsonian Tropical Research Institute.

The model was then compared to results from a study by Pierce et al. (2002) measuring carbon assimilation and C3-CAM behavior in a lab setting during drought. In this study, well-watered *G. monostachia* plants were placed in a controlled environment, with temperatures of 28/22°C (light/dark period), relative humidity of 60/90% (light/dark period), a photosynthetic photon fluence rate (PPFR) of 300 μmol/(m^2 s) at plant height for a photoperiod of 12 hours, and no precipitation input (Pierce et al., 2002). Similar to the experimental set-up, the model simulated the same environmental conditions, and began with a well-watered plant (x_w= 1.0) and an empty tank (x_t= 0). Because only 10% of carbon assimilation occurred at night, the plants were modeled as C3 plants.

2.5 Dry-down Simulation

A simulation of the epiphyte model was run to demonstrate the water use of the plant under drought conditions. For the dry-down of the epiphyte, with results given in Section 3.2, the model was run for one week with no precipitation input. The epiphyte began with a full tank (x_t= 1.0) and full internal plant capacitance (x_w= 1.0), and was simulated as a C3 plant with hydraulic and photosynthetic parameters for *G. monostachia* (see Tables 1 and 2). Although the epiphyte model was parameterized to C3 photosynthesis, the model was also run with CAM photosynthesis (using the existing C3 parameters) to demonstrate the qualitative CAM behavior from the model. To show the long-term behavior without the impacts of variations in daily weather, the solar radiation and atmospheric temperature were the repeated daily averages of the month of February of 1995 from the Lutz meteorological tower on Barro Colorado Island, Panama (weather data obtained from the Physical Monitoring Program of the Smithsonian Tropical Research Institute), and the relative humidity was kept constant at 90%.

2.6 Application to Rainforest Canopy

As an example of an application of the epiphyte model, and to understand how epiphytes may respond to varying environmental conditions within a rainforest canopy microclimate, the model was run with varying environmental inputs that simulated the vertical weather profiles within the canopy. The model was run as a C3 plant in a dry-down simulation with a full initial external tank (x_t= 1.0) and internal plant capacitance (x_w= 1.0). The environmental inputs, shown in Figure 4, were measured in February 2010 at the Lutz meteorological tower on Barro Colorado Island, Panama (obtained from the Physical Monitoring Program of the Smithsonian Tropical Research Institute) at canopy heights of 1 m (ground-level), 20 m, 42 m, and 48 m (top of canopy). Since the solar radiation was only measured at 48 m, the solar radiation at 48 m was adjusted by a factor to estimate the radiation at lower heights based on a similar observed canopy profile from Kumagai et al. (2001).

3 Results and Discussion

3.1 Parameterization with *G. monostachia*

Figure 5 shows the observed changes in transpirational water stress of *G. monostachia* for a 12-day rainless period during the 1995 dry season in Barro Colorado Island, Panama (Zotz & Andrade, 1997) compared to the model transpiration results using the parameterizations from Tables 1 and 2. Figure 5 also shows the percent error between the daily observations and model results. In comparison to the observed results, the modeled results show a similar decrease in transpiration rates, with a progressive decrease within 4-5 days, and similar minimum transpiration rates. The model generally shows similar behavior to the water loss curve from Zotz and Andrade (1997). The model overestimation on the first day may be due to the assumption that the plants started with a completely full internal plant capacitance (x_w = 1.0), even though the actual capacitance may have been slightly less than 1.0. After the initial decrease, the modeled transpiration rates responded to daily fluctuations in environmental inputs reasonably well. However, due to

the uncertain weather data (the specific start date of the experiment was not specified in Zotz and Andrade (1997)), the model match to the observed data is uncertain. In addition, if the plants in the experiment exhibited some CAM behavior, the results may be different, since they were modeled with C3 photosynthesis.

Figure 6 shows the observed changes in carbon assimilation of *G. monostachia* for a 6-day dry period under lab conditions (Pierce et al., 2002) compared to the modeled carbon assimilation results using C3 photosynthesis and the parameterizations from Tables 1 and 2. Figure 6 also shows the percent error between the maximum daily observed assimilation and the maximum daily model assimilation. Both the model and observed data show carbon assimilation rates of 3-4 μmol/(m^2 s), which is below the maximum carbon assimilation rate for *G. monostachia* of 4.67 μmol/(m^2 s) determined by Males and Griffiths (2018). In comparison to the observed results, the modeled results show a slower decrease in peak carbon assimilation rates, and lower carbon assimilation rates integrated over each day. In the original study, the plants exhibited approximately 10% CAM behavior, which is shown by the small peaks in assimilation during the night in Figure 6, which is not shown in the modeled results, since the plants were modeled as C3 plants.

3.2 Dry-down of an Epiphyte

The results from the simulation show temporal estimates of carbon assimilation, water fluxes, tank free-surface evaporation, and plant transpiration during a 7-day dry-down of an epiphyte for both C3 photosynthesis (Figure 7) and CAM photosynthesis (Figure 8). The results of this simulation characterize the general hydrologic behavior of epiphytes from the model.

For both photosynthetic pathways, tank storage (x_t) decreases as evaporation (E) and uptake from the tank into the plant (q_t) occur. Due to increased temperature and solar radiation, more free-surface evaporation occurs during the day, until it stops when the tank is empty. For CAM photosynthesis, some uptake from the tank into the plant occurs at night when carbon assimilation is occurring.

The tank is completely empty after 1 day for C3 photosynthesis and 2 days for CAM photosynthesis. The number of days it takes for the full tank to empty is within the range determined experimentally by Zotz and Thomas (1999), but is lower than the average value from the study. The time it takes for a full tank to dry out is lower in this model than in the results of Zotz and Thomas (1999) likely because this model does not apply an empirical adjustment accounting for the reduction in evaporation due to the protection from the epiphyte leaves. Figures 7 and 8 also show internal plant capacitance storage (x_w) and flux (q_w) for the dry-down. When there is water in the tank during the first few days, there is minimal flux from the internal plant capacitance, and then flux increases as water is withdrawn from the plant capacitance under increasing water stress.

Figures 7 and 8 show transpiration (T, mm/d per unit ground area) for the 7-day dry-down for C3 and CAM photosynthesis, respectively. For the C3 pathway, transpiration occurs during the daytime, and for the CAM pathway, transpiration also occurs at night when carbon assimilation occurs. The transpiration rates are significantly higher when the epiphyte tank has water. The leaf water potential remains high when there is water in the tank since the tank water has a water potential of 0 MPa, and then begins to decrease as transpiration occurs with an empty tank. The results from Figures 7 and 8 agree with typical behavior in epiphytes characterized by rapid water uptake during and immediately after precipitation events and low rates of water loss between events, as described by Zotz (2016). For this specific simulation, there was no absorption of atmospheric water vapor (q_h). When the atmospheric specific humidity is higher than the leaf specific humidity, which usually occurs under higher water stresses and more humid environments, the model results show an absorption of atmospheric water vapor.

Figures 7 and 8 also show carbon assimilation (A_n, μmol/(m^2 s) per unit leaf area) for the C3 and CAM pathways. The C3 carbon assimilation results in Figure 7 show carbon assimilation during the daytime. The CAM carbon assimilation results in Figure 8 reflect the typical daily CAM cycle, which is characterized by the majority of the carbon assimilation occurring at night, followed by a peak in carbon assimilation during the early morning, when the stomata remain open for the continued net uptake of CO_2 (Bartlett et al., 2014; Winter & Smith, 1996). A small amount of carbon assimilation also occurs in the evening, when the stomata open to uptake atmospheric CO_2 that is immediately utilized in the Calvin cycle (Bartlett et al., 2014). Since the model was

parameterized for a C3 plant, the magnitude of carbon assimilation in the CAM simulation is higher than expected, but can be adjusted in future studies when more CAM experimental data is available. Similar to transpiration, the carbon assimilation rates are higher when the epiphyte tank has water. The low stomatal conductances in Figures 7 and 8 agree with Zotz (2016), who observes that epiphytes tend to have a low stomatal conductance, and thus low transpiration rates.

Previous studies are lacking experimental observations of photosynthetic and hydraulic behavior of epiphytes in the transition between when there is water in the external tank and when the tank is empty. The epiphyte model presented in this study shows distinct behavior in the two phases, but the behavior with water in the tank and the transition to an empty tank has not yet been verified with experimental data. Nonetheless, the model still shows the expected behavior of a plant under stressed and non-stressed conditions. Detailed studies of epiphytes that exhibit full CAM photosynthesis are also missing in current research. In future studies, the epiphyte model can be used in tandem with experiments to formulate new hypotheses and better understand epiphyte tank water use behavior.

3.3 Application to Vertical Canopy Profiles

Figure 9 shows the simulation results of daily transpiration rates (T, mm/d per unit ground area) and water use efficiency (mmol$_{CO_2}$ assimilated per mol$_{H_2O}$ transpired) at canopy heights of 1, 20, 42, and 48 m when the rainforest canopy environmental inputs from Figure 4 were applied to the model. The application of the vertical profiles of canopy microclimatic inputs show that transpiration rates generally increase with increasing canopy height when the plant begins the simulation well-watered, which is a result of the higher solar radiation and temperature higher in the canopy. As the plant dries out, the epiphytes located lower in the canopy show more stable transpiration rates, while the epiphytes in the upper canopy show rapidly decreasing transpiration rates. Water use efficiency is higher for plants at lower heights throughout the simulation. The varying rates of transpiration are consistent with the observed vertical distribution of epiphytes in the canopy. Zotz (2016) observes that most epiphytes grow at heights of 5-20 m in a 40 m tall

rainforest, which corresponds to the results from this simulation that show that the plants at lower heights have more stable transpiration rates and higher water use efficiencies.

3.4 Implications for Microclimate and Earth System Modeling

The unique hydraulic processes of epiphytes have been shown to have effects on rainforest canopy microclimate. The presence of epiphytes as shade-providers and water reservoirs impact the temperature and humidity in the canopy. Within the rainforest canopy, epiphytes behave as a capacitor, dampening the daily fluctuations in atmospheric humidity and temperature (Freiberg, 2001; Stanton et al., 2014). In a study of a tropical forest during the late dry season, Stuntz et al. (2002) found that the total evapotranspiration from tree crowns with epiphytes, including epiphyte evapotranspiration, is less than the total evapotranspiration from tree crowns without epiphytes. The study also showed that within a single tree crown, vascular epiphytes provide microsites with lower temperatures and less evapotranspiration than do areas without epiphytes (Stuntz et al., 2002). The model presented in this paper provides a first step in integrating these epiphytic impacts on microclimate into a plant model. Through future epiphyte modeling advancements, the complex feedbacks between epiphytes, their host vegetation, the atmosphere can be further explored.

As vegetation components of Earth system models become more advanced, integrating epiphytic behavior, as outlined in this study, may help to improve estimates of water fluxes on both a global and local scale. Although the total biomass of epiphytes in rainforests is unknown, vascular epiphytes constitute an average of 20% and a maximum of 35-50% of the foliar biomass in rainforests of past studies (Lüttge, 2004; Nadkarni, 1984; Zotz, 2016), and contribute up to 13% of forest net primary production (Richardson et al., 2000). Epiphytes may account for a similar portion of the water budget in rainforests. Given rainforests provide approximately 30% of global evapotranspiration (Schlesinger & Jasechko, 2014), epiphytes could contribute up to approximately 3-6% of total terrestrial evapotranspiration, a significant water flux for Earth system modeling.

Further development of Earth system models could benefit from the integration of specific epiphytic characteristics. Liu et al. (2020) highlighted the importance of integrating plant hydraulics into Earth system models to more accurately estimate transpiration in response to atmospheric moisture stress, but the integration of epiphyte hydraulics has not yet been explored. A study that compares current Earth system model performance with and without the integration of an epiphyte model is needed to quantify the impacts that epiphyte modeling could have on the accuracy of water fluxes. Or and Lehmann (2019) integrated a canopy interception component to estimate global surface evaporation based on the leaf area index and a maximum water layer thickness on leaves. Mu et al. (2011) modified the MODIS evapotranspiration algorithm by including nighttime transpiration (i.e., cuticular transpiration), and evaporation from the water intercepted by the surface of the canopy. More detailed models, such as the one presented in this work, which models nighttime transpiration (i.e., CAM photosynthesis) and both free-surface evaporation and plant uptake from canopy interception, could help to produce a better physical representation of evapotranspiration in hydrological and climate models. Both the magnitude and timing of transpiration from the canopy could be different in this model than in traditional plant models. In addition, the volume of intercepted precipitation stored in the canopy may experience quicker uptake in the epiphyte model, in which the water can be used for transpiration, unlike traditional plant models. In addition, the integration of a plant system without soil into the Earth system models could impact microclimatic atmospheric humidity due to uptake from epiphytes, and may have impacts on the estimated soil moisture as well.

4 Conclusions

This work introduces a new model that represents epiphyte water use behavior. The epiphyte model, for the first time, presents a physiologically based vascular plant system model without soil. Using the Photo3 model that represents both C3 and CAM photosynthesis, the model applies environmental inputs to a big-leaf, numerical water balance model, with the Farquhar et al. (1980) model for photosynthetic carbon demand, an optimal control model for stomatal conductance, and a resistor-capacitor model of the plant-atmosphere continuum for plant hydraulics. Hydraulic

characteristics unique to epiphytes, including external tank storage, absorption of atmospheric humidity, succulent properties, and omission of root uptake from soil, are integrated into the model. The parameterized model results show some agreement with simulations of *G. monostachia* under drought conditions, but further validation is needed to characterize epiphyte water use when under well-watered conditions, when transitioning between conditions with full and empty external tank storage, and when exhibiting full CAM photosynthetic behavior. When forced with vertical profiles of environmental inputs measured within the rainforest canopy, the results of the model show increasing transpiration rates and decreasing water use efficiency with increasing canopy height. The modeled optimal water use efficiency at low to mid canopy heights agrees with the higher observed frequency of epiphytes at low to mid heights in rainforests.

The results of this work demonstrate the first step towards a more accurate quantification of epiphyte water fluxes. In the future, the epiphyte model can be integrated into Earth system models to help produce more reliable estimates of transpiration and free-surface evaporation from canopy. As climate change and sustainable water use become more pressing issues in the future, ecohydrological models, including this epiphyte model, will be helpful in quantifying the hydraulic behavior of plants and global water fluxes.

Appendix A: Specific Humidity

Following Jones (1992), the specific humidity of the leaf (q_l) can be calculated as

$$q_l(T_l, \psi_l) = q_{l\,sat}(T_l)\ \exp\left[\frac{V_w\ \psi_l}{R\ T_l}\right], \tag{15}$$

where $q_{l\,sat}$ is the saturated specific humidity at leaf temperature (T_l), V_w is the partial molar volume of water, ψ_l is the water potential of the leaf, and R is the universal gas constant.

The saturated humidity (q_{sat}) is related to the temperature (T) by (Jones, 1992)

$$q_{sat}(T) = \frac{0.622}{p_a}\ a_{sat}\ \exp\left[\frac{b_{sat}(T-273)}{c_{sat}+T-273}\right], \tag{16}$$

where q_{sat} is the saturated specific humidity at temperature T in Kelvin, p_a is atmospheric pressure (Pa), and a_{sat}, b_{sat}, and c_{sat} are empirical constants given in Table 3.

Appendix B: Conductances

Following Daly et al. (2004), the plant conductance (g_p) is modeled by a vulnerability curve, i.e.,

$$g_p = g_{p\,max}\ \exp\left[-\left(\frac{-\psi_l}{j}\right)^h\right], \tag{17}$$

so that g_p is near $g_{p\,max}$ for high ψ_l and is close to 0 for low ψ_l, since g_p drops when the water potential is too low because of xylem cavitation. The shape parameters j and h are both equal to 2 (Hartzell et al., 2018).

The internal storage conductance (g_w), is modeled in a similar manner to the plant conductance (g_p), i.e.,

$$g_w = g_{w\,max}\ \exp\left[-\left(\frac{-\psi_w}{j}\right)^h\right], \tag{18}$$

To simplify the model, and because the water potential of the water in the tank is always 0, the tank conductance (g_t) is set to a constant value when there is water in the tank (see Table 1), and 0 when the tank is empty.

Following Jones (1992), the stomatal conductance for water (g_s) is closely related to the stomatal conductance for CO_2, i.e.,

$$g_s = 1.6\, g_{s\,CO_2} + g_{cut}, \tag{19}$$

where $g_{s\,CO_2}$ is the stomatal conductance for CO_2 (see Photo3 model (Hartzell et al., 2018) for details on calculations) and g_{cut} is the cuticular conductance, which accounts for the small amount of water vapor lost when carbon assimilation is not occurring.

The conductance of the absorption of atmospheric water vapor (g_h) was assumed to be similar in magnitude to the cuticular conductance (g_{cut}).

The atmospheric conductance (g_a) is a function of wind speed and canopy height (Jones, 1992), i.e.,

$$g_a = \frac{u_z\, k^2}{(\ln[(z-d)/z_o])^2}, \tag{20}$$

where u_z is the wind speed, k is the Von Karman constant, z is the height of the wind speed measurement, d is 0.64 * canopy height, and z_o is 0.13 * canopy height.

Appendix C: Water Potentials

Since the water in the tank is free-standing water, it is assumed to have a water potential (ψ_t) of 0 MPa.

The plant water potential (ψ_w) is the sum of the osmotic and turgor pressure, following the method given by Bartlett et al. (2014). The plant osmotic pressure (Ω) is given by (Hem, 1985)

$$\Omega = \frac{RT_l}{V_w}\, \ln\left(\frac{n_w}{n_w + n_s}\right), \tag{21}$$

where R is the ideal gas constant, T_l is the leaf temperature (K), V_w is the molar volume of liquid water (m^3/mol), n_s is the total moles of solute, and n_w is the total moles of water, on a total leaf area basis (mol/m^2). The total moles of water is given by

$$n_w = \frac{x_w Z_w}{V_w}, \tag{22}$$

where x_w is the relative plant capacitance fraction, Z_w is the maximum water storage capacitance, and V_w is the molar volume of liquid water. The osmotic pressure when the plant is well-watered (x_w = 1, full turgor) is determined by the total moles of solute (n_s), which is assumed to be a constant for simplicity. The osmotic potential of epiphytes is usually at a lower magnitude (-1 MPa) than water stressed terrestrial plants because in the absence of soil, a more negative osmotic

potential is not needed to drive water uptake during short pulses of water availability (Zotz & Hietz, 2001). When the plant is well-watered, the osmotic pressure is balanced by the turgor pressure. The plant turgor pressure (Π) is given by a power law equation (Ranney et al., 1990), i.e.,

$$\Pi = (x_w - d_1)^{d_2}, \tag{23}$$

where x_w is the relative plant capacitance fraction, and d_1 and d_2 are fitted values based on observed pressure-volume data from Zotz and Andrade (1997) (see Figure 3).

Acknowledgements

G.M. acknowledges support from the Adler Independent Work/Senior Thesis Fund from the School of Engineering and Applied Science of Princeton University, and Princeton Environmental Institute's Undergraduate Research Fund for senior thesis research. A.P. acknowledges support from the US National Science Foundation (NSF) grants EAR-1331846 and EAR-1338694 and the Carbon Mitigation Initiative at Princeton University. Data sets provided by the Physical Monitoring Program of the Smithsonian Tropical Research Institute.

Conflict of Interest

No conflict of interest was declared.

Data Availability Statement

The epiphyte model software can be accessed at https://github.com/gretamiller/Epiphyte. It was developed in Python 3.7 by Greta Miller, Samantha Hartzell, and Amilcare Porporato, and first made available in 2020. It was built off of the Photo3 photosynthesis model for rooting plants,

which can be accessed at https://samhartz.github.io/Photo3/. Additional data that support the findings of this study are available upon request.

References

Bartlett, M. S., Vico, G., & Porporato, A. (2014). Coupled carbon and water fluxes in CAM photosynthesis: modeling quantification of water use efficiency and productivity. *Plant and Soil*, *383*, 111–138. https://doi.org/10.1007/s11104-014-2064-2

Benz, B. W., & Martin, C. E. (2006). Foliar trichomes, boundary layers, and gas exchange in 12 species of epiphytic Tillandsia (Bromeliaceae). *Journal of Plant Physiology*, *163*, 648–656. https://doi.org/10.1016/j.jplph.2005.05.008

Buckley, T. N., & Schymanski, S. J. (2014). Stomatal optimisation in relation to atmospheric CO2. *New Phytologist*, *201*, 372–377. https://doi.org/https://doi.org/10.1111/nph.12552

Daly, E., Porporato, A., & Rodriguez-Iturbe, I. (2004). Coupled Dynamics of Photosynthesis, Transpiration, and Soil Water Balance. Part I: Upscaling from Hourly to Daily Level. *Journal of Hydrometeorology*, *5*(3), 546–558. https://doi.org/10.1175/1525-7541(2004)005<0546:CDOPTA>2.0.CO;2

Farquhar, G. D., Caemmerer, S. V., & Berry, J. A. (1980). A biochemical model of photosynthetic CO2 Assimilation in Leaves of C3 Species. *Planta*, *149*, 78–90. https://doi.org/10.1007/BF00386231

Freiberg, M. (2001). The influence of epiphyte cover on branch temperature in a tropical tree. *Plant Ecology*, *153*, 241–250. https://doi.org/https://doi.org/10.1023/A:1017540629725

Hartzell, S., Bartlett, M. S., & Porporato, A. (2017). The role of plant water storage and hydraulic strategies in relation to soil moisture availability. *Plant and Soil*, *419*, 503–521. https://doi.org/10.1007/s11104-017-3341-7

Hartzell, S., Bartlett, M. S., & Porporato, A. (2018). Unified representation of the C3, C4, and CAM photosynthetic pathways with the Photo3 model. *Ecological Modelling*, *384*, 173–187. https://doi.org/10.1016/j.ecolmodel.2018.06.012

Hem, J. D. (1985). *Study and Interpretation of the Chemical Characteristics of Natural Water* (tech. rep.). Department of the Interior, US Geological Survey.

Holbrook, N. M., & Putz, F. E. (1996). From epiphyte to tree: Differences in leaf structure and leaf water relations associated with the transition in growth form in eight species of hemiepi-

phytes. *Plant, Cell and Environment*, *19*, 631–642. https://doi.org/10.1111/j.1365-3040.1996.tb00398.x

Hunt, E. R., Running, S. W., & Federer, C. A. (1991). Extrapolating plant water flow resistances and capacitances to regional scales. *Agricultural and Forest Meteorology*, *54*, 169–195. https://doi.org/10.1016/0168-1923(91)90005-B

Jarvis, A. (2000). *Quantifying the hydrological role of cloud deposition onto epiphytes in a tropical montane cloud forest, Colombia* (Doctoral dissertation). King's College London.

Jones, H. G. (1992). *Plants and Microclimate: A Quantative Approach to Environmental Plant Physiology*. Cambridge University Press.

Katul, G. G., Palmroth, S., & Oren, R. (2009). Leaf stomatal responses to vapour pressure deficit under current and CO2-enriched atmosphere explained by the economics of gas exchange. *Plant, Cell and Environment*, *32*, 968–979. https://doi.org/10.1111/j.1365-3040.2009.01977.x

Kumagai, T., Kuraji, K., Noguchi, H., Tanaka, Y., Tanaka, K., & Suzuki, M. (2001). Vertical profiles of environmental factors within tropical rainforest, Lambir Hills National Park, Sarawak, Malaysia. *Journal of Forest Research*, *6*, 257–264. https://doi.org/10.1007/BF02762466

Liu, Y., Kumar, M., Katul, G. G., Feng, X., & Konings, A. G. (2020). Plant hydraulics accentuates the effect of atmospheric moisture stress on transpiration. *Nature Climate Change*, *10*, 691–695. https://doi.org/10.1038/s41558-020-0781-5

Lüttge, U. (2004). Ecophysiology of Crassulacean Acid Metabolism (CAM). *Annals of Botany*, *93*, 629–652. https://doi.org/10.1093/aob/mch087

Males, J., & Griffiths, H. (2018). Economic and hydraulic divergences underpin ecological differentiation in the Bromeliaceae. *Plant Cell and Environment*, *41*, 64–78. https://doi.org/10.1111/pce.12954

Martin, C. E., & Schmitt, A. K. (1989). Unusual water relations in the CAM atmpospheric epiphyte Tillandia usneoides L. (Bromeliacae). *Botanical Gazette*, *150*, 1–8.

Medlyn, B. E., Duursma, R. A., Eamus, D., Ellsworth, D. S., Barton, C. V., Crous, K. Y., De Angelis, P., Freeman, M., & Wingate, L. (2011). Reconciling the optimal and empirical

approaches to modelling stomatal conductance. *Global Change Biology*, *17*, 2134–2144. https://doi.org/https://doi.org/10.1111/j.1365-2486.2010.02375.x

Mu, Q., Zhao, M., & Running, S. W. (2011). Improvements to a MODIS global terrestrial evapotranspiration algorithm. *Remote Sensing of Environment*, *115*, 1781–1800. https://doi.org/10.1016/j.rse.2011.02.019

Nadkarni, N. M. (1984). Epiphyte Biomass and Nutrient Capital of a Neotropical Elfin Forest. *Biotropica*, *16*, 249–256.

Nobel, P. S., & Jordan, P. W. (1983). Transpiration Stream of Desert Species: Resistances and Capacitances for a C3, a C4, and a CAM plant. *Journal of Experimental Botany*, *34*, 1379–1391. https://doi.org/10.1093/jxb/34.10.1379

North, G. B., Browne, M. G., Fukui, K., Maharaj, F. D., Phillips, C. A., & Woodside, W. T. (2016). A tale of two plasticities: leaf hydraulic conductances and related traits diverge for two tropical epiphytes from contrasting light environments. *Plant Cell and Environment*, *39*, 1408–1419. https://doi.org/10.1111/pce.12697

Or, D., & Lehmann, P. (2019). Surface evaporative capacitance – how soil type and rainfall characteristics affect global scale surface evaporation. *Water Resources Research*, *55*, 519–539. https://doi.org/10.1029/2018WR024050

Pierce, S., Winter, K., & Griffiths, H. (2002). Carbon isotope ratio and the extent of daily CAM use by Bromeliaceae. *New Phytologist*, *156*, 75–83. https://doi.org/10.1046/j.1469-8137.2002.00489.x

Pypker, T. G., Unsworth, M. H., & Bond, B. J. (2006). The role of epiphytes in rainfall interception by forests in the Pacific Northwest. II. Field measurements at the branch and canopy scale. *Canadian Journal of Forest Research*, *36*, 819–832. https://doi.org/10.1139/x05-286

Ranney, T. G., Whitlow, T. H., & Bassuk, N. L. (1990). Response of five temperate deciduous tree species to water stress. *Tree Physiology*, *6*, 439–448. https://doi.org/10.1093/treephys/6.4.439

Richardson, B. A., Richardson, M. J., Scatena, F. N., & McDowell, W. H. (2000). Effects of nutrient availability and other elevational changes on bromeliad populations and their inverte-

brate communities in a humid tropical forest in Puerto Rico. *Journal of Tropical Ecology*, *16*, 167–188. https://doi.org/10.1017/S0266467400001346

Schlesinger, W. H., & Jasechko, S. (2014). Transpiration in the global water cycle. *Agricultural and Forest Meteorology*, *189-190*, 115–117. https://doi.org/10.1016/j.agrformet.2014.01.011

Schmitt, A., Martin, C. E., & Lüttge, U. E. (1989). Gas Exchange and Water Vapor Uptake in the Atmospheric CAM Bromeliad Tillandsia recurvata L.: The Influence of Trichomes. *Botanica Acta*, *102*, 80–84. https://doi.org/10.1111/j.1438-8677.1989.tb00070.x

Silvera, K., & Lasso, E. (2016). Ecophysiology and crassulacean acid metabolism of tropical epiphytes. *Tropical Tree Physiology: Adaptations and Responses in a Changing Environment* (pp. 25–43). Springer International Publishing. https://doi.org/10.1007/978-3-319-27422-5_2

Stanton, D. E., Huallpa Chávez, J., Villegas, L., Villasante, F., Armesto, J., Hedin, L. O., & Horn, H. (2014). Epiphytes improve host plant water use by microenvironment modification. *Functional Ecology*, *28*, 1274–1283. https://doi.org/10.1111/1365-2435.12249

Stuntz, S., Simon, U., & Zotz, G. (2002). Rainforest air-conditioning : the moderating influence of epiphytes on the microclimate in tropical tree crowns. *International Journal of Biometerology*, *46*, 53–59. https://doi.org/10.1007/s00484-001-0117-8

Tyree, M. T., & Ewers, F. W. (1991). Tansley Review No . 34 The hydraulic architecture of trees and other woody plants. *New Phytologist*, *119*, 345–360.

Winter, K., & Smith, J. (1996). An Introduction to Crassulacaean Acid Metabolism. Biochemical Principles and Ecological Diversity. *Ecological studies* (114th ed., pp. 1–13). Springer.

Winter, K., & Holtum, J. A. (2014). Facultative crassulacean acid metabolism (CAM) plants: Powerful tools for unravelling the functional elements of CAM photosynthesis. *Journal of Experimental Botany*, *65*, 3425–3441. https://doi.org/10.1093/jxb/eru063

Zotz, G. (2004). How prevalent is crassulacean acid metabolism among vascular epiphytes? *Oecologia*, *138*, 184–192. https://doi.org/10.1007/s00442-003-1418-x

Zotz, G. (2016). *Plants on Plants – The Biology of Vascular Epiphytes*. Springer International Publishing. https://doi.org/10.1007/978-3-319-39237-0

Zotz, G., & Andrade, J. (1997). Water Relations of Two co-Occuring Epiphytic Bromeliads. *Journal of Plant Physiology*, *152*, 545–554.

Zotz, G., & Hietz, P. (2001). The physiological ecology of vascular epiphytes: current knowledge, open questions. *Journal of Experimental Botany*, *52*, 2067–2078. https://doi.org/10.1093/jexbot/52.364.2067

Zotz, G., & Thomas, V. (1999). How much water is in the tank? Model calculations for two epiphytic bromeliads. *Annals of Botany*, *83*, 183–192. https://doi.org/10.1006/anbo.1998.0809

Table 1: Plant hydraulic parameters for *G. monostachia*

Parameter	Value	Units	Description
LAI	3.0[a]	m^2_{leaf} / m^2_{ground}	Leaf area index
TAI	0.17[b]	m^2_{tank} / m^2_{ground}	Tank area index
Z_t	0.015[b]	m	Maximum tank storage depth
Z_w	0.0027[b, c]	m	Maximum plant capacitance depth
g_a	12[d]	mm/s	Atmospheric conductance per unit ground area, Eq. 20
$g_{p\,max}$	0.076[e]	μm/(s MPa)	Maximum plant conductance per unit leaf area
$g_{w\,max}$	0.0045[f]	μm/(s MPa)	Maximum internal storage conductance per unit leaf area
g_{cut}	0.01[g]	mm/s	Cuticular conductance per unit leaf area
g_h	0.01[g]	mm/s	Conductance of the absorption of atmospheric water vapor per unit leaf area
g_t	0.5[h]	μm/(s MPa)	Tank conductance
f	0.5[f]	–	Relative height of plant capacitance
h	2[f]	–	Shape parameter for Eq. 17 and 18
j	2[f]	–	Shape parameter for Eq. 17 and 18
d_1	0.0[i]	–	Shape parameter for Eq. 22
d_2	2.0[i]	–	Shape parameter for Eq. 22
n_s	1.1[i]	mol/m^2	Shape parameter for Eq. 23

[a] Based on reasonable estimate of similar species
[b] Based on Zotz and Thomas (1999)
[c] Based on Zotz and Andrade (1997)
[d] Based on Jones (1992) for a wind speed of 0.75 m/s at 2 m altitude, with a plant height of 0.5 m
[e] Based on North et al. (2016)
[f] Based on estimate from Hartzell et al. (2018)
[g] Based on Zotz (2016)
[h] Estimate within range of soil conductances for rooting plants
[i] Fitted to pressure-volume curve from Zotz and Andrade (1997)

Table 2: Photosynthetic parameters for *G. monostachia*

Parameter	Value	Units	Description
ψ_{LA0}	-1.0[a]	MPa	Point of maximum plant water stress
ψ_{LA1}	-0.3[a]	MPa	Onset of plant water stress
$V_{c,max0}$	10.4[b]	μmol/(m^{2}s)	Maximum carboxylation rate
$J_{c,max0}$	20.8[b]	μmol/(m^{2}s)	Electron transport rate
M_{max}	152[b]	mol/m^3	Maximum malic acid concentration

[a] Parameters for CAM species in Hartzell et al. (2018), adjusted to fit observed data
[b] Parameters for CAM species in Hartzell et al. (2018), reduced by factor of 0.8 to fit observed data

Table 3: Fixed Constants

Parameter	Value	Units	Description
a_{sat}	613.75[a]	–	Constant for Eq. 16
b_{sat}	17.502[a]	–	Constant for Eq. 16
c_{sat}	240.97[a]	–	Constant for Eq. 16
p_a	101,325	Pa	Atmospheric pressure
λ_w	$2.5*10^6$	J/kg	Latent heat of vaporization
ρ_a	1.27	kg/m^3	Air density
ρ_w	998	kg/m^3	Water density
c_p	1012	J/(kg K)	Specific heat of air
R	8.314	J/(mol K)	Universal gas constant
V_w	$1.81*10^5$	m^3/mol	Molar volume of water
k	0.41	–	Von Karman constant

[a] Based on Jones (1992)

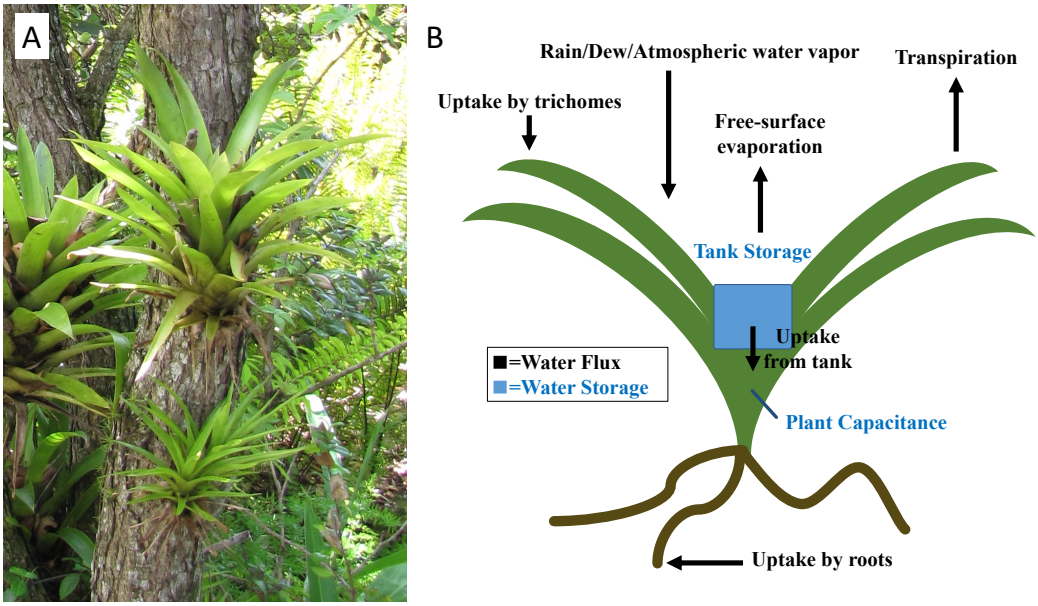

Figure 1: (A) Photograph of *Guzmania monostachia* in Maui, Hawaii (photo by Forest and Kim Starr, under Creative Commons License: https://creativecommons.org/licenses/by/2.0/deed.en). (B) Water balance of an epiphyte, where the water fluxes are labeled in black and the water storages are labeled in blue.

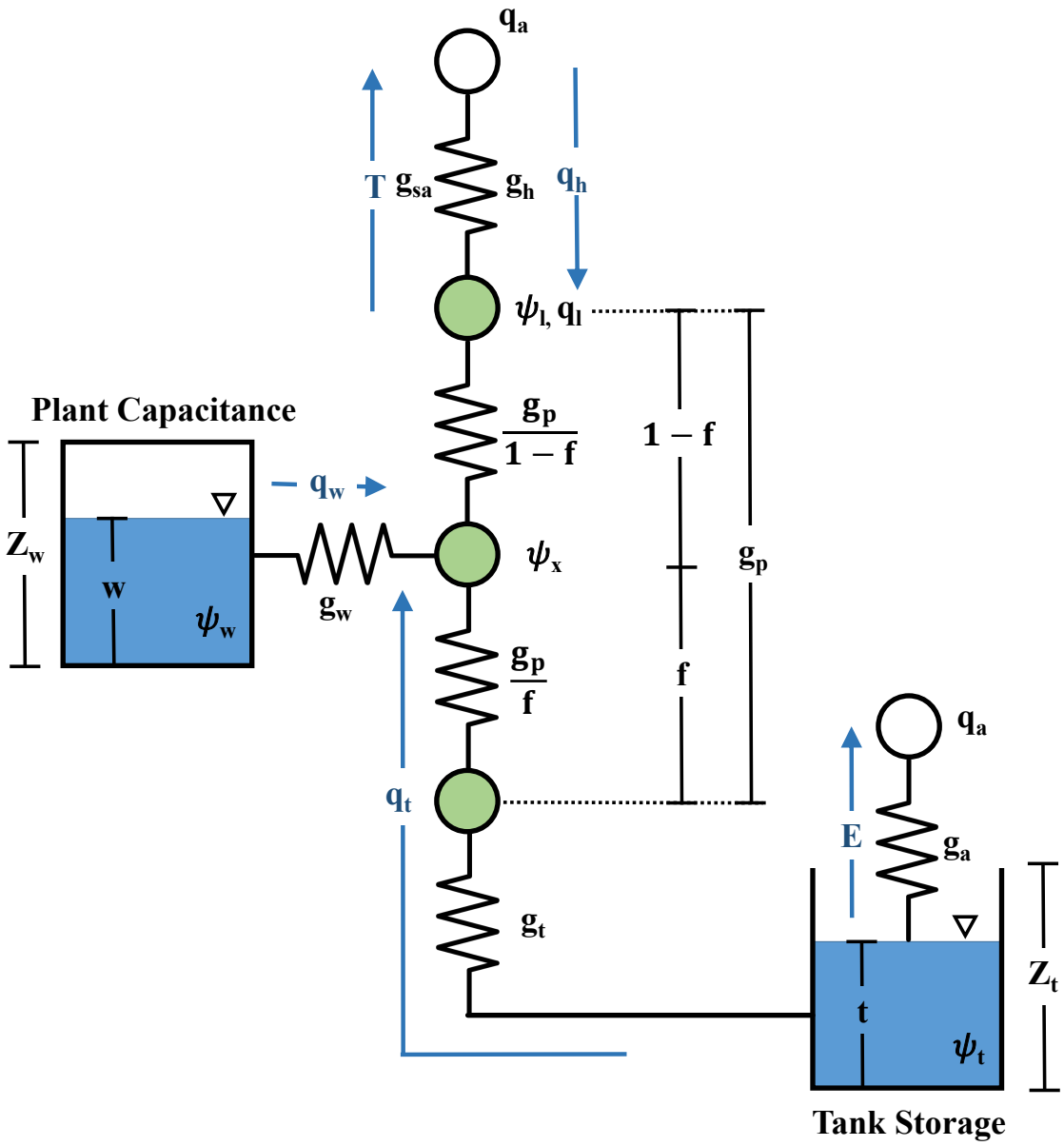

Figure 2: Model schematic of water fluxes and storages for epiphytes. Water from the tank storage, with a maximum height of Z_t, and water from internal plant capacitance, with a maximum height of Z_w, moves along a water potential gradient, through the plant, and into the atmosphere with humidity q_a. The fluxes of water, including flux from tank (q_t), flux from internal plant capacitance (q_w), are equivalent to the conductance (g) multiplied by the difference in water potential (ψ) between each pair of nodes of the plant. The transpiration from the epiphyte (T), absorption of atmospheric water vapor (q_h), and evaporation from the tank storage (E) are equivalent to the conductance (g) multiplied by the difference in specific humidity between the surface and the atmosphere.

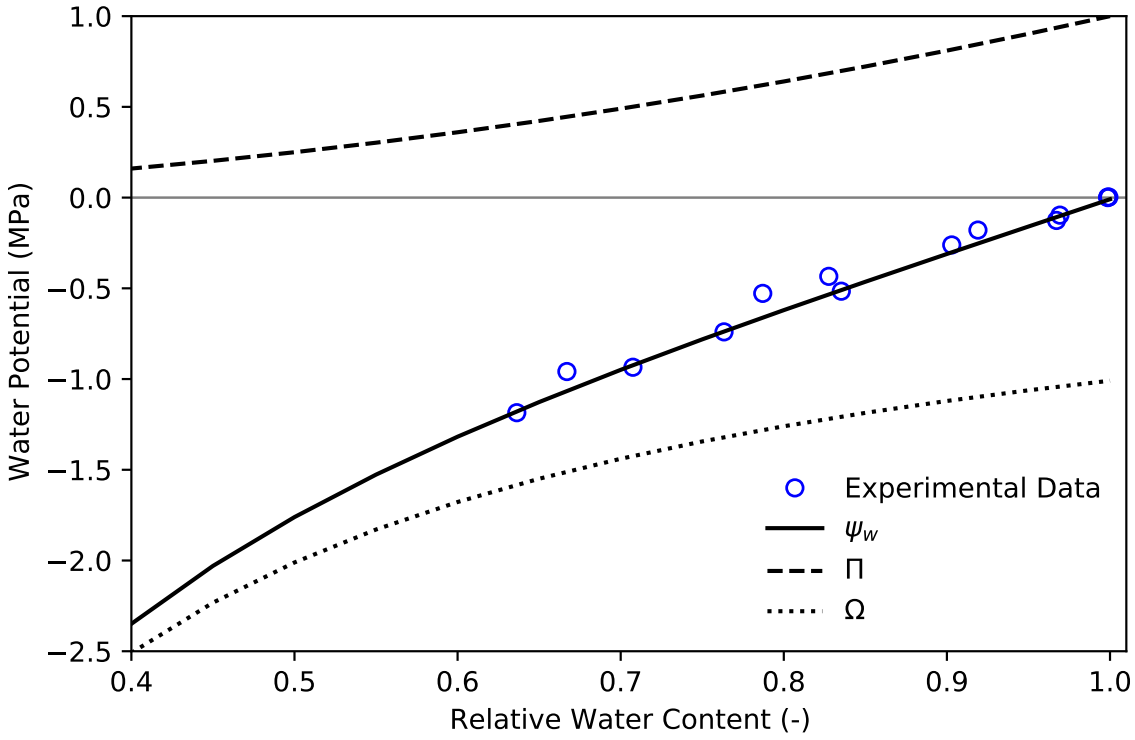

Figure 3: Pressure-volume curve for *G. monostachia*. The solid line is a fit to the data from Zotz and Andrade (1997) using a nonlinear plant capacitance equation (See Appendix C). The water potential (ψ_w) is the sum of the osmotic pressure (Ω) and turgor pressure (Π).

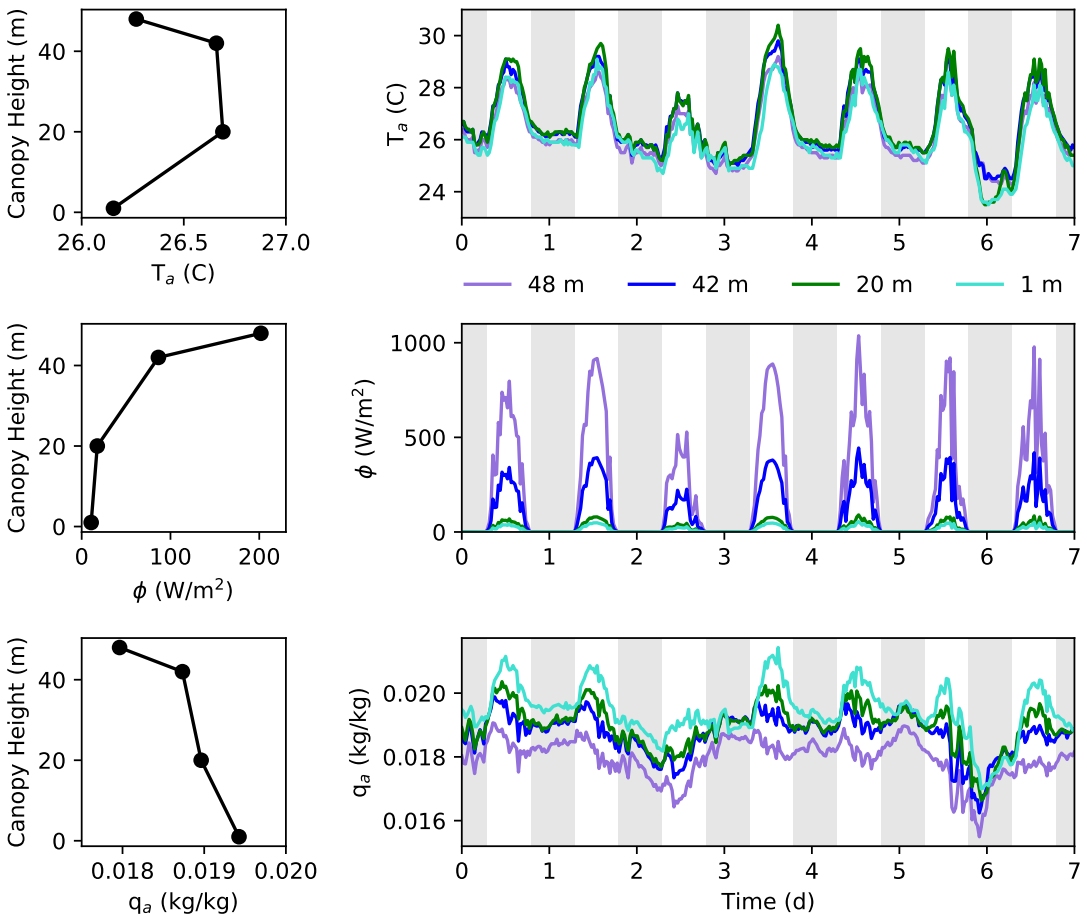

Figure 4: Environmental inputs at different heights within the canopy. Atmospheric temperature (T_a), solar radiation (ϕ), and atmospheric humidity (q_a) vary throughout time with canopy height. Data are from the first week of February 2010 from the Lutz meteorological tower on Barro Colorado Island, Panama (Physical Monitoring Program of the Smithsonian Tropical Research Institute).

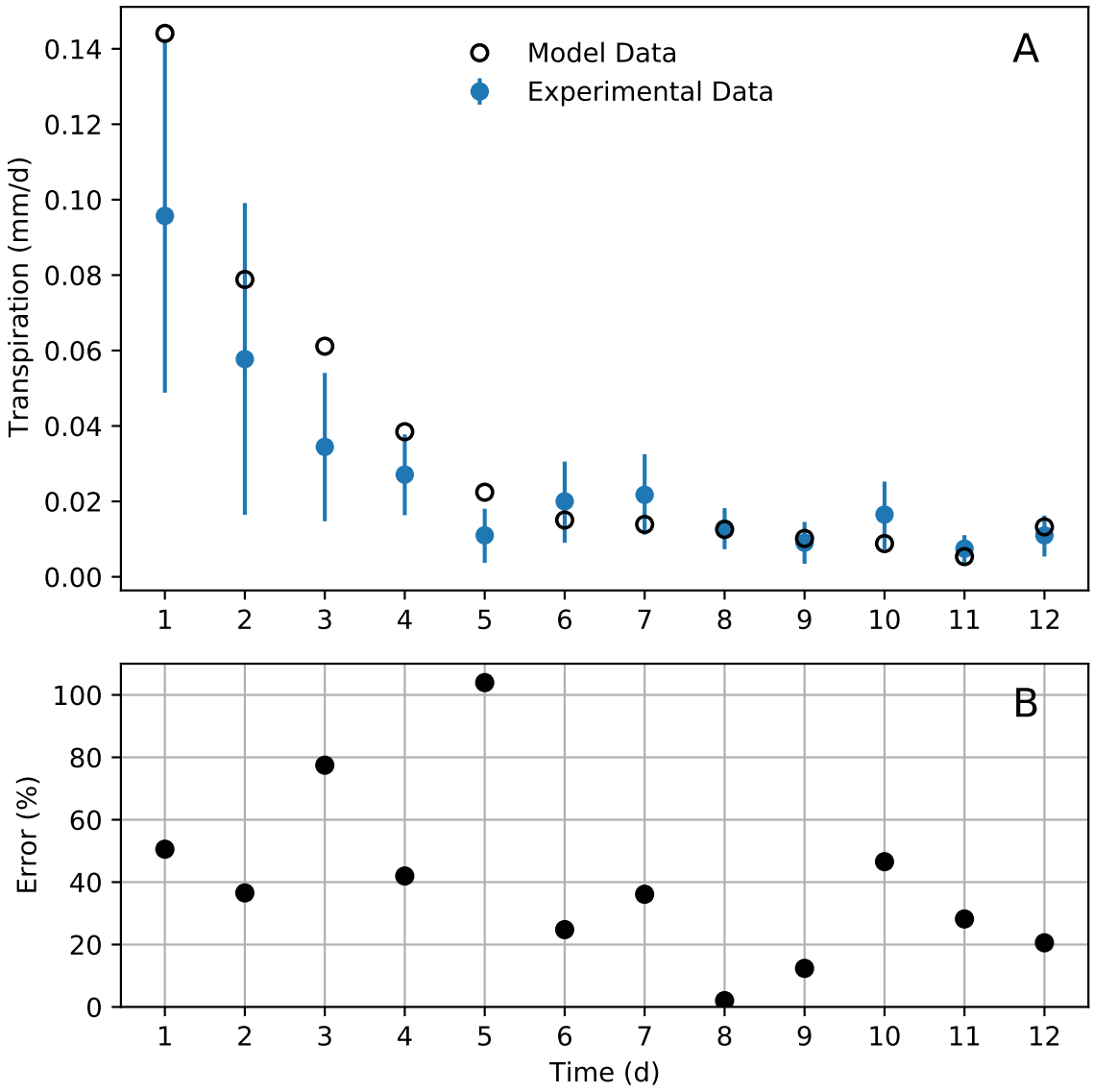

Figure 5: (A) Observed changes in transpirational water stress of *G. monostachia* for a 12-day rainless period during the 1995 dry season in Barro Colorado Island, Panama (Zotz & Andrade, 1997) in comparison to the model transpiration results. The observed data are daily means ± SD for 16 plants, in mm/d per unit leaf area. (B) Percent error in daily transpiration between model and experimental data.

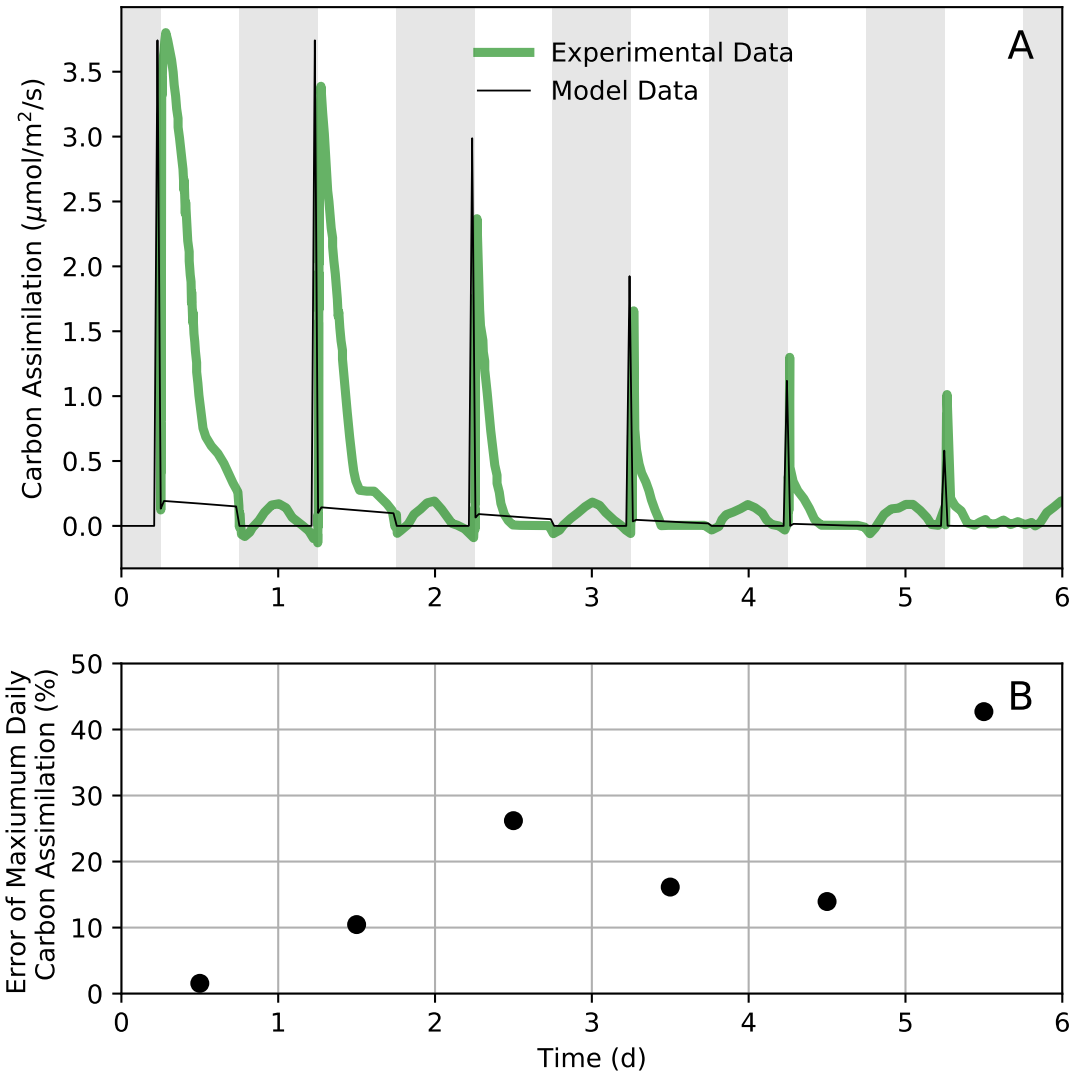

Figure 6: (A) Observed changes in carbon assimilation of *G. monostachia* for a 6-day dry period under lab conditions (Pierce et al., 2002) in comparison to the model carbon assimilation results with C3 photosynthesis. The carbon assimilation rates are measured per unit leaf area. (B) Percent error in peak daily assimilation between model and experimental data.

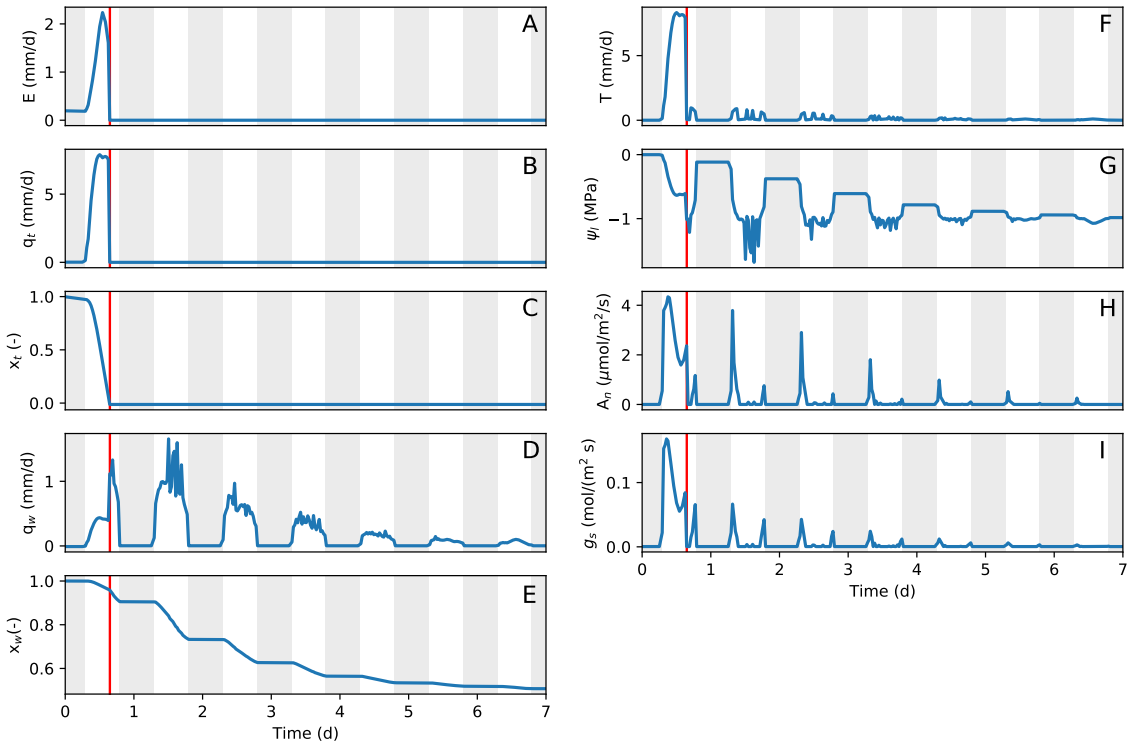

Figure 7: Model results for a 7-day dry-down of an epiphyte with C3 photosynthesis, starting with a full tank and full plant capacitance. (A) Free-surface evaporation from tank (E, mm/d per unit ground area). (B) Uptake by the epiphyte from the tank storage (q_t, mm/d per unit ground area). (C) Relative tank storage (x_t). (D) Flux between internal plant storage and xylem (q_w, mm/d per unit ground area). (E) Relative plant capacitance (x_w). (F) Transpiration (T, mm/d per unit ground area) for a 7-day dry-down of an epiphyte, starting with a full tank and full plant capacitance. (G) Leaf water potential (ψ_l, MPa). (H) Carbon assimilation (A_n, μmol/(m^2 s) per unit leaf area). (I) Stomatal conductance (g_s, mol/(m^2 s)). The vertical gray bars indicate nighttime, the vertical white bars indicate daytime, and the red line indicates the time when the tank fully emptied.

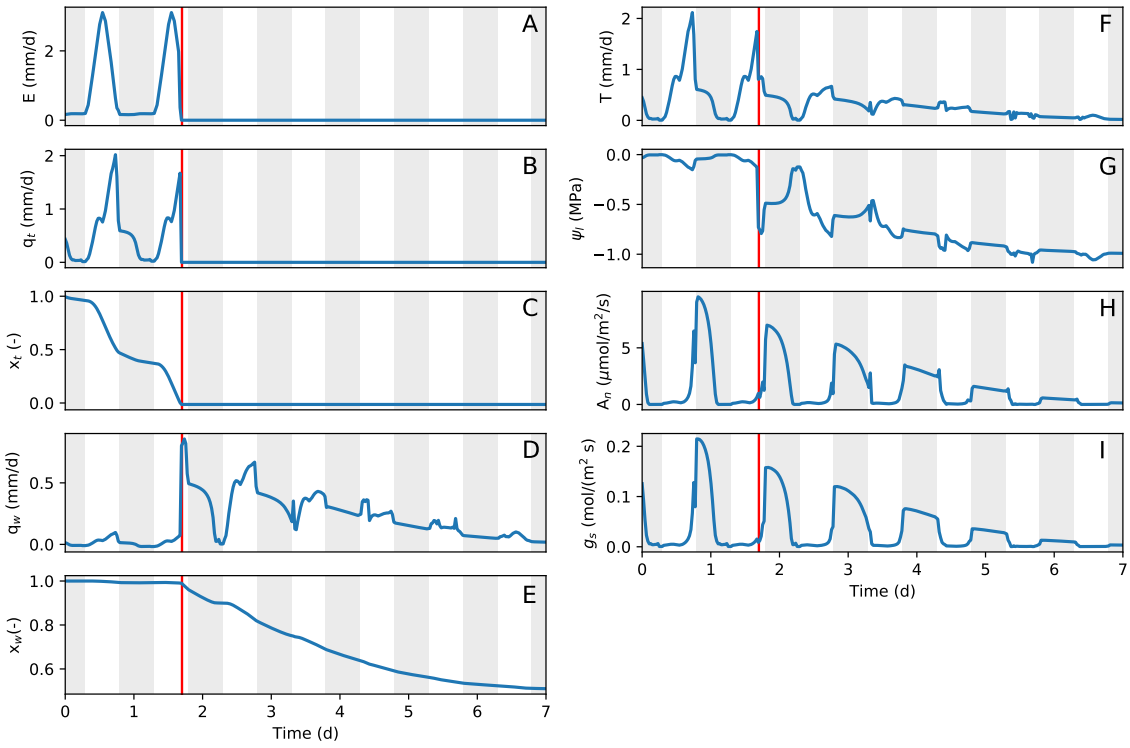

Figure 8: Model results for a 7-day dry-down of an epiphyte with CAM photosynthesis, starting with a full tank and full plant capacitance. (A) Free-surface evaporation from tank (E, mm/d per unit ground area). (B) Uptake by the epiphyte from the tank storage (q_t, mm/d per unit ground area). (C) Relative tank storage (x_t). (D) Flux between internal plant storage and xylem (q_w, mm/d per unit ground area). (E) Relative plant capacitance (x_w). (F) Transpiration (T, mm/d per unit ground area) for a 7-day dry-down of an epiphyte, starting with a full tank and full plant capacitance. (G) Leaf water potential (ψ_l, MPa). (H) Carbon assimilation (A_n, μmol/(m^2 s) per unit leaf area). (I) Stomatal conductance (g_s, mol/(m^2 s)). The vertical gray bars indicate nighttime, the vertical white bars indicate daytime, and the red line indicates the time when the tank fully emptied.

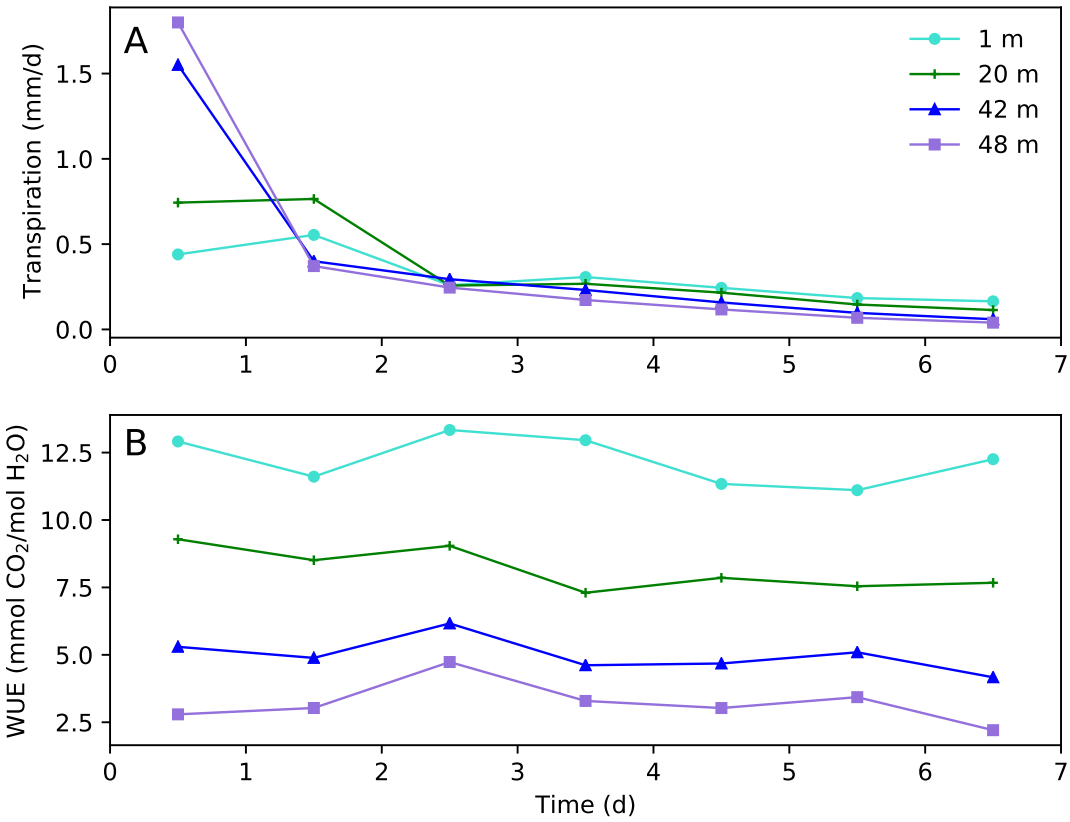

Figure 9: (A) Average daily transpiration rates (T, mm/d per unit ground area) and (B) average daily water use efficiency (WUE, mmol_{CO_2} assimilated per mol_{H_2O} transpired) at different heights within the rainforest canopy.